Opportunistic Packet Scheduling in Body Area Networks

K. Shashi Prabh[1] and Jan-Hinrich Hauer[2]

[1] Center for Real-Time Systems Research (CISTER)
School of Engineering (ISEP)
Polytechnic Institute of Porto, Portugal
ksp@isep.ipp.pt
[2] Telecommunication Networks Group
Technische Universität Berlin, Germany
hauer@tkn.tu-berlin.de

Abstract. Significant research efforts are being devoted to Body Area Networks (BAN) due to their potential for revolutionizing healthcare practices. Energy-efficiency and communication reliability are critically important for these networks. In an experimental study with three different mote platforms, we show that changes in human body shadowing as well as those in the relative distance and orientation of nodes caused by the common human body movements can result in significant fluctuations in the received signal strength within a BAN. Furthermore, regular movements, such as walking, typically manifest in approximately periodic variations in signal strength. We present an algorithm that predicts the signal strength peaks and evaluate it on real-world data. We present the design of an opportunistic MAC protocol, named BANMAC, that takes advantage of the periodic fluctuations of the signal strength to achieve high reliability even with low transmission power.

1 Introduction

As the fraction of the aging population is increasing, the load on the healthcare services is also growing. Yet, there is a severe current and projected shortage of healthcare personnel. For example, a shortage of 1 million registered nurses by the year 2020 is projected within the USA alone [26]. Networks of sensors around as well as inside the human body, referred to as Body Area Networks (BAN), promise to revolutionize healthcare practices as they facilitate, among other things, better diagnosis, fast emergency response and personalized medication [12]. But although BANs have the potential to enable low-cost, personalized healthcare systems, it is still unclear whether they can meet the stringent QoS requirements imposed by some applications. To limit the interference to neighboring BANs and to keep the specific absorption rate (SAR) as low as possible in the interest of protecting the human tissues, it is desirable that the transmission power be kept low. The error-proneness of the low-power wireless communication, however, is a major challenge. Although the distances between devices in

BANs are usually small, the wireless signal may experience severe attenuation from human body shadowing [17]. Furthermore, the changes in the environment as well as relative distance and orientation of the devices resulting from human mobility can introduce significant variations in the quality of the wireless signal.

We begin this paper with an experimental investigation of the signal strength dynamics within a BAN during periodic human movements, such as walking. We observe that the periodic changes in the relative positions of the limbs typically manifest in significant periodic changes in received signal strength (of several dBs). Furthermore, the signal strength amplitudes are typically long-lasting, of the order of 100s of milliseconds, when compared to the airtime of packets, which are of the order of only a few milliseconds. To exploit this effect we propose BANMAC, a MAC protocol that is built on the idea of opportune packet transmission, that is, packets are scheduled such that they are transmitted when signal strength is high, because then the chances are better that the packets are received correctly.

The main contributions of this paper are:

1. An empirical characterization of RSSI fluctuations in a BAN while the subject is walking *outdoors*. This work is complimentary to some of the studies done by the IEEE 802.15.6 working group in *indoors* settings [6]. Contrary to the indoors study [6], we did not always find significant differences in RSSI measurements due to internal versus external antenna. Specifically, the node placements where body shadowing is significant resulted in no significant difference.
2. The design and evaluation of an RSSI-based opportune transmission windows prediction algorithm.
3. BANMAC, a MAC protocol for BANs that schedules transmissions opportunistically when the link margin is likely to be higher than the average. We have designed BANMAC to be compatible with the recommendations of the IEEE 802.15.6 working group for MAC protocols in BANs.

The rest of this paper is organized as follows: in Sec. 2 we present a description of our experimental setups and report on typical signal strength fluctuations that we observed in BANs. We present the details and evaluations of an opportune transmission window prediction algorithm in Sec. 3. We then present BANMAC that is based on the idea of transmitting during high RSSI windows in Sec. 4. We discuss related work in Sec. 5 and conclude the paper in Sec. 6.

2 RSSI Measurements

This section describes our experimental setup and reports on typical RSSI fluctuations observable in a BAN when the subject is walking. We performed experiments with three different node platforms: Shimmer2, TelosB and MicaZ.

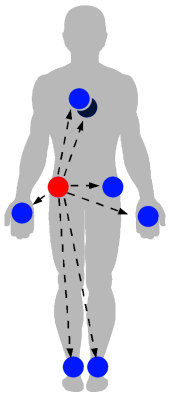

Fig. 1: Node positions: the sender is in the right pocket.

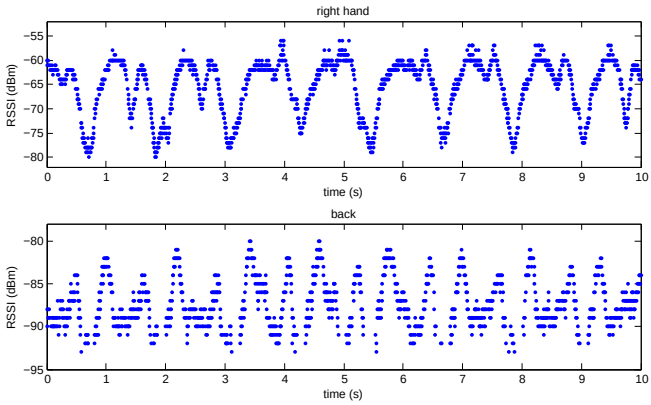

Fig. 2: RSSI measured on the right hand (top) and back (bottom) while the subject is walking.

2.1 Experimental Setup: Shimmer2

In our setup, a BAN consists of eight Shimmer2 [24] nodes. Like the popular Telos [23] platforms, Shimmer2 integrates the Texas Instruments MSP430 MCU and the IEEE 802.15.4-compliant CC2420 transceiver [4]. The Shimmer2 platform also incorporates a Bluetooth radio, but we don't use it. Our Shimmer2 nodes are also equipped with a 2 GB MiniSD card, which was sufficient to store all traces that accumulated during one set of experiments.

The nodes were positioned on the subjects as shown in Fig. 1. An experiment consisted of one node (*sender*) continuously broadcasting IEEE 802.15.4 packets with a constant transmission frequency of 200 Hz – one 14-byte (MPDU size) packet every 5 ms. The other seven nodes (*receivers*) were passively listening for these packets (they did not send acknowledgments). The sender used a transmission power of -10 dBm,[3] and it was always located in the right trouser pocket of the subject.[4] Our measurement software accesses the CC2420 radio directly, i.e., there is no MAC layer involved and the senders send packets immediately without clear channel assessment (CCA). Each of the seven receiver nodes keeps statistics of the number of correctly received packets and the associated Received Signal Strength Indicator (RSSI), which is measured using the first eight symbols following the start-of-frame delimiter (SFD) of the received packets [4]. The receiver nodes are placed on the left and right ankle, left trouser pocket, left and right hand, in the center of the chest, and in the center of the back (Fig. 1).

In each experiment the subjects walked continuously outdoors in a large park, an environment of negligible external RF interference, as we verified with

[3] The CC2420 supports a transmission power of 0 dBm, but previous work [13] has shown that -10 dBm often results in acceptable packet reception rates.

[4] In real life this node could be the user's cell phone, which is often carried around this location.

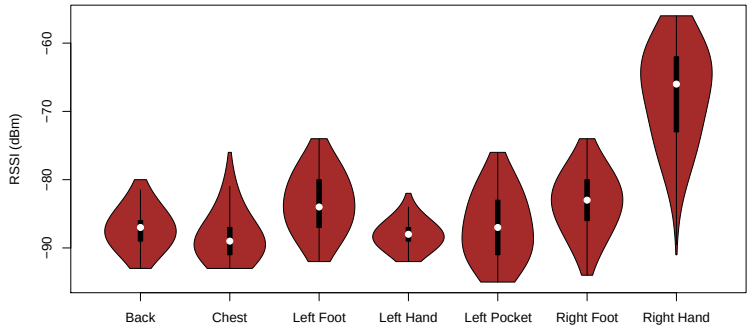

Fig. 3: Typical RSSI fluctuations during a 5-minute experiment.

the help of periodic noise-floor measurements on the nodes. The subjects were walking at the speed of approximately 1.2 steps/s, which is a typical walking speed. A single experiment lasted for 5 minutes (60,000 packets). Three different subjects performed 10 experiments each.

RSSI Fluctuations While a subject was walking, the changes in the relative positions of the limbs manifested as periodic fluctuations in the RSSI. For example, the top graph in Fig. 2 shows a 10-second snapshot of the RSSI obtained in one experiment on a node that was positioned on the right hand of the subject (recall that the sender is always located in the right trouser pocket). The graph shows a period of about 1.2 s, which matches the step frequency of the subject. It also shows the frequent occurrence of a plateau of about 1 s duration with RSSI values of −60 dBm followed by short trough with RSSI values as low as −80 dBm, corresponding to a significant RSSI range of approximately 20 dB. The node position, however, has an impact on the RSSI pattern: for example, the RSSI time series obtained in the same experiment on the back of the subject is much more noisy (Fig. 2 bottom).

Our goal is to exploit the RSSI fluctuations by scheduling packet transmissions such that they occur when the RSSI values are high, because then the chances are better that the packets are received correctly [25]. One precondition is that there is enough variance in the RSSI time series. To get an estimate of the magnitude of the RSSI fluctuations, we examined the RSSI inter-quartile ranges (IQR): for every 5-minute experiment we determined the distance between the 75th percentile and the 25th percentile of the RSSI readings per node position, which is essentially the range of the middle 50% of the data. Figure 3 summarizes the results in a violin plot (a combination of a boxplot and a kernel density plot), where the IQRs are shown as thin black boxes around the median (white dot). Thus the edges of the boxes represent the 25th and 75th percentiles. In this experiment the RSSI IQR varied between 2 and 9 dB. Note that RSSI values below the −94 dBm sensitivity threshold of the radio [4] are unavailable because these packets are typically dropped. Figure 3 can be regarded as a representa-

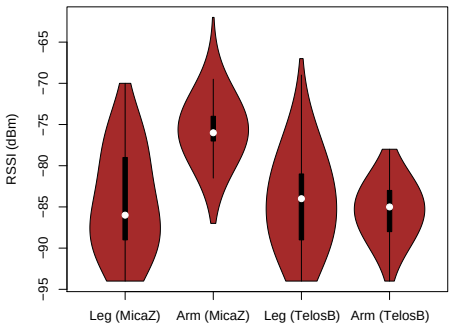

Fig. 4: Typical RSSI fluctuations on TelosB and MicaZ platforms.

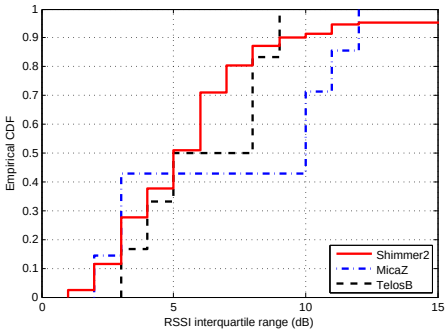

Fig. 5: CDF of the RSSI inter-quartile ranges.

tive example for the 10 experiments carried out by that specific subject, because in all experiments performed by a certain subject we found the corresponding median and IQR to be usually very similar.

The larger the RSSI IQR the more spread out are the RSSI values and thus the higher the potential for exploiting fluctuations by timely packet scheduling. Figure 5 shows a CDF of the RSSI IQR for all 30 experiments including the data of all three subjects. It can be seen that half of the links have an RSSI IQR of at least 5 dB and on 20% of the links the RSSI IQR is at least 8 dB.

2.2 Experimental Setup: MicaZ and TelosB Platforms

We repeated a set of similar experiments on the TelosB and MicaZ platform. Like Shimmer2, both platforms are also equipped with the CC2420 radio, but they have different antennas: while Shimmer2 has an SMD antenna, TelosB features inverted-F microstrip antenna and MicaZ features a half-wave dipole antenna. One of the goals was to investigate the differences arising due to different types of antennas. In these experiments we reduced the transmission rate to 20 packets/s and set the transmission power to -20 dBm. We used only one sender/receiver pair at a time. The sender was positioned on either the right foot or the right upper arm and the receiver was positioned on the chest. The receiver forwarded the received packets over the serial port to a laptop. The subject was walking at normal walking speed outdoors on a lawn.

In the following, we use MA to indicate the experiments with MicaZ nodes where the sender was placed on the upper arm and TA to indicate the same experiments where the nodes were TelosB motes. Similarly, we use ML to indicate the experiments with MicaZ nodes where the sender was placed on the leg and TL to indicate the same experiments where the nodes were TelosB motes. We also performed these experiments where the subject stood still, which we label as “MA Static” and so on.

RSSI Fluctuations Fig. 4 shows violin-plots of some representative results (again in all experiments performed by a given subject the median and IQR per node position are usually very similar) and Fig. 5 shows the IQR CDFs for the two platforms. We found an IQR link margin of approx. 5 dB for the chest-arm pairs and of approx. 10 dB for chest-leg pairs (Table 1). Thus, aside from some differences due to different transmission power levels, the RSSI IQRs on the TelosB and MicaZ platforms are similar to those obtained on the Shimmer2 platform, which confirms that the effect is not platform-specific, but a general one.

Due to mobility, the standard deviations of RSSI fluctuations increased by approx. 1 dB when the sender was placed on the upper arm (Table 1). This fluctuation increased to 2.9 dB for MicaZ and 1.4 dB for TelosB motes when the sender was placed on the leg. However, mobility does not necessarily results in the decrease of the mean or median of the RSSI fluctuations. Contrary to the indoor measurements reported in [6], we found comparable attenuation (in ML and TL configurations) using printed (TelosB) and dipole (MicaZ) antennas, which can be explained by the absence of multi-path receptions outdoors.

	RSSI			
Expt. Config.	Median Gain (dB)	IQR (dB)	Range (dB)	Std. Dev (dB)
MA	-51	4	31	2.81
MA Static	-55	2	27	1.79
TA	-65	5	17	3.68
TA Static	-62	5	21	2.87
ML	-65	12	26	6.19
ML Static	-62	4	21	3.33
TL	-64	9	37	5.56
TL Static	-67	7	20	4.11

Table 1: Summary of RSSI fluctuations.

2.3 Discussion

The RSSI fluctuations are influenced by several factors. The periodic changes in the relative positions of the limbs causes periodic differences in (1) relative node distance, which influences path-loss and fading, (2) shadowing and (3) relative node orientation. All these, in conjunction with the irregular antenna radiation pattern of the nodes, can result in different signal strength at the same distance. Our evaluation of the RSSI IQRs revealed that the magnitude of the RSSI fluctuation is usually position-dependent and often *significant* (several dB). In addition, the absolute RSSI values were often close to the sensitivity threshold of the radio, where even a small change in RSSI can result in a substantial difference

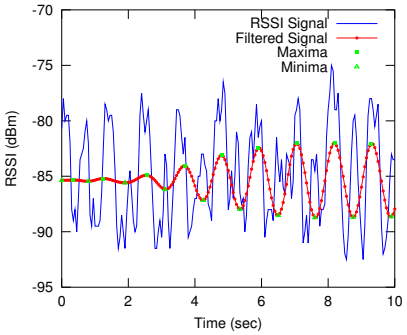

Fig. 6: Bandpass filtered RSSI signals – TelosB.

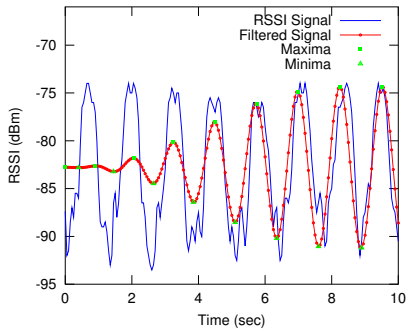

Fig. 7: Bandpass filtered RSSI signals – MicaZ.

in packet delivery performance [25]. However, in order to exploit any fluctuation, the RSSI pattern must also be *predictable*. Ideally, it should be periodic and maintain durable amplitudes as shown in the top graph in the top Fig. 2, because then the packets can be scheduled within the RSSI peak time windows and the packet losses can be reduced.

3 Opportune Transmission Windows

We use the term *opportune transmission window* (OTW) to describe a time interval that yields high RSSI values relative to the average RSSI of the link. Assuming that the subject performs regular movements, intuitively, we can predict an OTW by adding the current step period to the time of the previous OTW center. In this section we describe a method that derives both of these from RSSI time series obtained from a set of initial probe (control) packets.

3.1 RSSI-based OTW Prediction

The main difficulty in using RSSI measurements to predict opportune transmission windows arises due to significant noise content in the RSSI measurements (Section 2.1). The second challenge arises due to the irregularities of human movements, which are usually never exactly periodic. Consequently, the simplistic approach of locating the peaks and extrapolating the inter-peak separation to predict OTW fails. However, we observed that in the Fourier domain the dominant peak in the power spectrum of RSSI time series corresponds to the speed of the subject.

RSSI-based OTW Prediction Algorithm In order to find the OTW the sender transmits RSSI probe packets which are received at an appropriate node

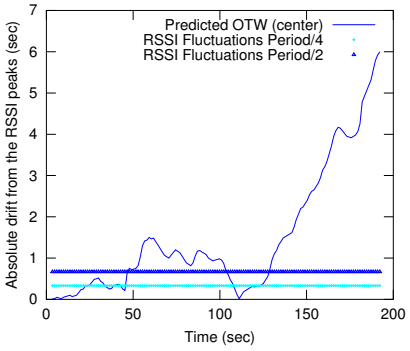

Fig. 8: Deviations of OTW predictions without dynamic correction.

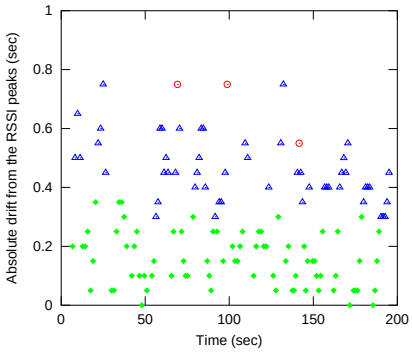

Fig. 9: Deviations of OTW predictions with periodic corrections: MicaZ sample.

specified by the coordinator. The probe packets are transmitted at (sufficiently) low frequency, interspersed between data packets. The receiver returns the RSSI values of the probe packets in aggregated form to the coordinator, possibly piggybacked on the data packets. The coordinator maintains a moving window of the RSSI time series. At the coordinator node, we apply Fast Fourier Transform (FFT) to the RSSI time series and find the dominant frequency. To determine the phase, we first apply a tight bandpass filter centered at the dominant frequency. Figures 6-7 show the filtered signal superimposed on samples of raw RSSI data. On the filtered signal, we then apply an extrema identification algorithm to determine the peaks. Since the RSSI sample has arbitrary phase at the two ends, we select the last but one peak as the basis for OTW predictions, to which we add integral multiples of the period (1/dominant frequency) for one set of nodes and odd half integral multiples of period for the other set of nodes, where the nodes on the left hand and right leg constitute one of the two sets, and symmetrically the nodes on the left hand and the right leg constitute the other. The first set is defined by the membership of the node that provides the RSSI samples. The rectification of the drifts in OTW predictions due to irregularities in the subject's movements can be done by re-running the algorithm either periodically or on-demand, for example, when significant deviation from the predictions are detected.

3.2 Evaluation

For evaluating the OTW prediction algorithm, we used the measurement data described earlier in Section 2.2. Our bandpass filter uses Butterworth filters. The filter pass frequencies were set to 0.1 Hz below and above the dominant frequency. The cutoff frequencies were 0 Hz and twice the central frequency. The passband ripple was set to 1 dB and the stopband attenuation was set to 30 dB.

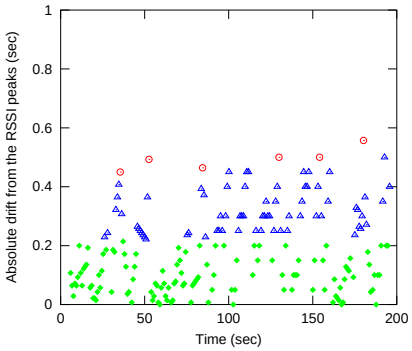

Fig. 10: Deviations of OTW predictions with periodic corrections: Shimmer2 sample.

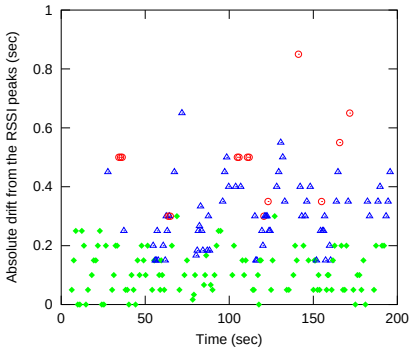

Fig. 11: Deviations of OTW predictions with periodic corrections: TelosB sample

Figure 8 shows the RSSI peak prediction drifts, or, the absolute difference between the peaks of the filtered RSSI signal and the center of predicted OTWs. For this figure, the expected times of RSSI peaks were obtained by adding multiples of the period obtained initially. The deviations are the differences of the nth RSSI peak prediction time and the actual nth peak observed in the filtered data. Due to varying pace, stopping and other irregularities in walking, the drift generally grows with time.

The next three figures (Fig. 9–11) show the absolute deviations between the center of predicted OTWs and the nearest bandpass filtered RSSI peaks observed in the experiments, when the predictions were periodically adjusted. We sampled RSSI periodically every 12 s and collected RSSI samples at 20 Hz for 4.5 s. In other words, we used approx. one-third of the RSSI time series to validate this algorithm. The sampling time of 4.5 s was chosen to ensure the inclusion of at-least one pair of consecutive RSSI peaks. In figures 9–11, the drifts less than $0.25 * period$ are shown with diamonds, those less than $0.5 * period$ and greater than $0.25 * period$ with triangles and the larger drifts with circles. The means of the absolute deviations were 0.28 s for the MicaZ samples, 0.21 s for the TelosB samples and 0.18 s for the Shimmer2 samples. In all three cases, the non-central node was on one of the legs.

We observed that both the probe frequency and the probe duration can be significantly reduced without sacrificing accuracy of predictions. The optimization of these parameters is one of our future work. We note that if the coordinator and at-least one of the nodes have more than one radio transceiver, such as in the Shimmer2 motes, then our OTW prediction method can also be applied using secondary radios.

4 BANMAC

In this section we illustrate the use of the work presented in the previous two sections. We present BANMAC, a MAC protocol for body area networks which attempts to schedule transmissions during the time windows when the RSSI is expected to be larger than average. Our network model consists of a set of nodes connected in star topology to a coordinator node where the coordinator is significantly more powerful than the rest of the nodes.

Similar to IEEE 802.15.4, BANMAC alternates between centralized and distributed medium access modes. In the centralized mode, where the scheduling decisions are made by the coordinator, the channel access is collision-free and the MAC protocol supports features such as priority and guaranteed data rate. In the distributed scheduling mode of BANMAC, the nodes determine the time windows for opportunistic transmissions locally and contend for channel access during these windows. We describe the centralized scheduling algorithm of BANMAC in the following subsection (4.1). A detailed presentation of BANMAC will appear in a separate publication.

4.1 Centralized BANMAC Scheduling

Opportune Transmission Windows (OTW).

Recall that we use the term *opportune transmission window* (OTW) to describe a time interval that yields high RSSI values relative to the average RSSI of the link, for example, the time interval of 3.5 s to 4.0 s in the top graph in Fig. 2. Assuming that the period and phase of the RSSI fluctuations are known (we describe an algorithm that derives this information from the RSSI time series in the previous section), let T be the period of RSSI fluctuations. Let $t = 0$ correspond to the start of the positive half-cycle (zero phase) for some node i as shown in Fig. 12. Then, the OTWs of node i span $[nT + (T/4 - \Delta/2), nT + (T/4 + \Delta/2))$ where n is an integer and Δ is the width of the OTWs. The left hand and right leg move in synchrony, and so do the other pair. Due to the synchronous and alternating motion of the pair of limbs, the time axis contains alternating OTWs, each OTW for the set of nodes on the two limbs that move together. These are shown as $\Delta(S_1)$ and $\Delta(S_2)$ in the figure, where node i belongs to the set S_1. Observe that $\Delta(S_1)$ and $\Delta(S_2)$ need not overlap. The gaps may be used for communication with nodes whose RSSI do not exhibit periodic fluctuations and for distributed medium access.

Scheduling

We associate a cost function with the time of transmissions where the minima of the cost function coincide with the center of the OTWs. In the following, we present an algorithm that minimizes the cost of a set of transmissions. We adapt the Gravitational Task Model of Guerra and Fohler [10] to solve this problem. Their work is inspired from the physical system of a set of pendulums

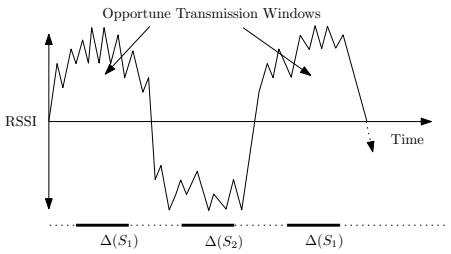

Fig. 12: Opportune transmission windows alternate for the two sets of nodes S_1 and S_2, explained in the text.

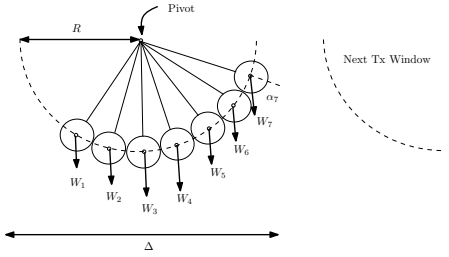

Fig. 13: Pendulum task model

in equilibrium (Fig. 13), where the equilibrium is characterized by the minimum total potential energy of the set of pendulums.

Problem Formulation. Let us consider a set of n transmissions $\mathcal{T} = \{X_1, \ldots X_n\}$ to be scheduled during a given opportune transmission window, where X_i denotes the events of polling by the coordinator followed by the transmission of data packet to the coordinator. It may be that a number of data packets are sent to the coordinator following one poll packet. For the sake of simplicity of presentation, we treat the transmission of m data packets in succession as m single transmissions. Let $t_{\mathcal{T}}$ denote the center of the OTW and let Δ denote the width of the OTW. Let w_i denote the numerical measure of the importance of X_i. Finally, let e be the time needed to complete a single transmission event, X_i.

We map our problem formulation to a Gravitational Task Model instance as follows: we consider a set of n pendulums hanging from a pivot (Fig. 13). A bob in the pendulum system corresponds to one transmission. The diameter of the bobs (the same for all bobs) map to the transmission duration e. The weights of the pendulums correspond to the importance of transmissions. Furthermore, the swing range $2R$ maps to the width of OTW (minus a correction term), $\Delta - e$.[5] Table 14 presents a summary of the mappings.

The potential energy of a bob is U_i = weight * vertical displacement from the minimum $= -W_i\sqrt{R^2 - x_i^2}$ where x_i is the horizontal deviation of the bob from the central position, that is, the horizontal deviation from the projection of $t_{\mathcal{T}}$ (Fig. 15). The minimization of the potential energy can be expressed as the following nonlinear program (NLP):

$$\text{Minimize} \quad \sum_{i=1}^{n} -W_i\sqrt{R^2 - x_i^2}, \tag{1}$$

$$\text{subj. to} \quad x_{i+1} - x_i = e, \; i = 1, \ldots n-1, \tag{2}$$

$$\text{where} \quad |x_i| \leq R, \; i = 1, \ldots n-1. \tag{3}$$

[5] We have simplified the model presented in [10] by redefining R as above.

Pendulum		Opportunistic Transmissions	
Name	Symbol	Name	Expression
Pivot	P	Target Tx time	$t_{\mathcal{T}}$
Weight of bob	W_i	Importance	w_i
Diameter of bob	e	Tx duration	e
Swing range	$2R$	Opportune Tx window	$\Delta - e$

Fig. 14: Mapping of opportunistic transmissions parameters to Gravitational Task Model.

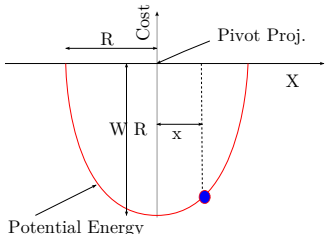

Fig. 15: Cost at displacement x from pivot (OTW center) in the Gravitational Task Model.

In Equation 2, the equality sign (rather than $\geq$) is chosen because all transmissions within any given window have the same target transmission time, and hence, the optimal solution can't have gaps. We solve this NLP in *linear time-complexity* by using the physical facts that in equilibrium, the bobs touch each other and the net torque on the system is zero. The interested reader is referred to [10] for more details. A transmission schedule is given by the projection of bobs on a horizontal line below the pendulums. However, the projections, if not corrected, overlap. In the following, we find expressions for the projections of the center of bobs sufficiently shifted such that the projections of the bobs do not overlap.

Minimum cost schedule. Let α_i be the angle that pendulum i makes with the vertical (Fig. 13). Then the displacement of the center of the bob along the X-axis is $x_i = R\sin\alpha_i$. Thus, we get

$$R\sin\alpha_{i+1} - R\sin\alpha_i = e,\ \forall i \tag{4}$$

$$\sum_{i=1}^{n} W_i R\sin\alpha_i = 0. \tag{5}$$

Eqn. 4 can be re-written as:

$$R\sin\alpha_i = R\sin\alpha_n - (n-i)e. \tag{6}$$

Substituting (6) in (5), we get the expression for the displacement of the last bob in equilibrium:

$$R\sin\alpha_n = \frac{\sum_{i=1}^{n-1}(n-i)eW_i}{\sum_{i=1}^{n} W_i} \tag{7}$$

The conditions $\sin\alpha_n > (1 - \frac{e}{2R})$ in (7) and $\sin\alpha_1 < -(1 - \frac{e}{2R})$ in (6) indicate the unschedulability of $\mathcal{T}$ within the opportune transmission window.

Examples. Let us consider a set of four pendulums, which models a set of four transmissions, say $\mathcal{T}$, to be scheduled in a given OTW. From (7), we get,

$$x_4 = R\sin\alpha_4 = \frac{e(3W_1 + 2W_2 + W_3)}{W_1 + W_2 + W_3 + W_4}. \tag{8}$$

Consider the case of equal weight bobs, i.e., $W_i = W\ \forall i$. Then, the displacement of the fourth pendulum from the center is $R\sin\alpha_4 = 1.5e$. We use (6) to get the displacements of other pendulums. The displacement of the third pendulum is $R\sin\alpha_3 = 0.5e$, that of the second pendulum is $R\sin\alpha_2 = -0.5e$ and that of the first pendulum is $R\sin\alpha_1 = -1.5e$. Thus the first transmission is scheduled at $t_{\mathcal{T}} - 2e$, the second transmission is scheduled at $t_{\mathcal{T}} - e$ and so on. Now suppose $W_1 >> W_i,\ i = 2, 3, 4$. Then, from (8), $R\sin\alpha_4 \cong 3e$, which corresponds to the case of pendulum 1 being almost at the center as expected.

The work presented in [10] (and Equation 4) minimizes the cost function for a given ordering of transmissions. From symmetry, the ordering that maximizes the number of schedulable transmissions corresponds to the ordering where the "center of mass" is located in the middle. However, the possibility of performing such orderings is limited by the start time constraints and transmission order dependencies.

5 Related Work

Several studies have focused on the effects of human body shadowing on RF communication. Kara et al. describe an experimental study that evaluates attenuation due to people crossing a 2.4 GHz band link [15]. They show that the human body can result in attenuation of up to 20 dB. Shadowing effects caused by a human body have been studied in [8] for 802.11 radios. There are also several studies that focus on human body shadowing at other frequencies. For example, the 900 MHz and 60 GHz bands are the focus of [18] and the 10 GHz band is the focus of [9].

Due to its focus on low-power communication, the work of Miluzzo et al. [17] is closely related to ours. The authors performed an experimental study in which they investigate person-to-person communication with IEEE 802.15.4 radios. Their results indicate that the position of the radio on the human body as well as the attenuation introduced by the human body has a significant effect on the performance of the communication. The experimental part of our work can be regarded complementary as we have focused on intra-BAN communication only. Some of the work presented in IEEE 802.15.6 WG proceedings is also related to ours. Davenport et al. present a study of link characterization of medical BAN indoors [6]. In [2], Cai et al. derive a two state channel model based on empirical RSSI measurements in BANs, which also match our experimental results. A MAC protocol for BANs is proposed in [30], where throughput maximization is the objective. To the best of our knowledge, our work is the first to propose the idea of opportunistic transmission scheduling exploiting RSSI fluctuations for better reliability.

Like BANs, energy efficiency is one of the main concerns in Wireless Sensor Networks (WSN). A number of energy efficient MAC protocols have been proposed for WSNs. Putting nodes to sleep is the primary mechanism for energy saving in S-MAC [28] and T-MAC [5]. Their main difference is the use of fixed versus variable sleep cycles (see [11] for a comparative study) . Since all receivers

listen during wake-up periods when the energy spent while not receiving transmissions is wasted, low power listening (LPL) at the receivers improves energy efficiency. Berkeley-MAC [19], WiseMAC [7] and X-MAC [1] use this paradigm. Large latency is a critical problem with this approach. X-MAC improves energy efficiency of B-MAC and WiseMAC by strobing the long preambles and inserting receiver ID in the strobes. An early CTS in X-MAC alleviates the latency problem. CMAC [16] also tries to improve the LPL latency. However, the protocol has the overhead of synchronizing time slots. Scheduled channel polling (SCP) [29] eliminates the need for long preambles in LPL by synchronized polling. At the time of polling, a sender wakes up the receiver and after performing a short carrier sense, it transmits the packet. SCP has been found to decrease the limiting duty cycle LPL from 1-2% to 0.1%. TDMA based MAC protocols can offer bounded delays and collision-free transmissions. TRAMA [20] is a collision-free TDMA MAC protocol for WSN. ZMAC [22] is a hybrid MAC protocol, that operates in CSMA mode under light load conditions and in TDMA mode under heavy load conditions.

Targeted scheduling of tasks have been studied before by the real-time systems research community. Time Value Functions (TVF) or, Time Utility Functions (TUF) express the value of the completion of a task as a function of time. Jensen et al. proposed the use of TVFs for real-time process scheduling [14]. Chen and Muhlethaler present a heuristic to schedule tasks that attempts to maximize the sum of TVF for each task [3]. Wang and Ravindran improve the heuristic of Chen and Muhlethaler from $O(n^3)$ time complexity to $O(n^2)$ time complexity [27]. See [21] for a survey.

6 Conclusion

In an experimental study conducted with three different mote platforms, we showed that regular human movements often manifest in significant periodic RSSI fluctuations. We presented and evaluated an algorithm that predicts opportune transmission windows and deals with irregularities of human movements and noisy RSSI signals. We also presented a sketch of a MAC protocol for BANs, named BANMAC, that takes advantage of these fluctuations by opportunistically scheduling transmissions when the RSSI is likely to be higher than the average, for better reception reliability. In an ongoing work, we are integrating BANMAC to the IEEE 802.15.4 protocol stack. We plan to extend our work to incorporate dynamic power control and channel migration in the near future.

Acknowledgments

This research was partially supported by the European Commission under contract number FP7-2007-IST-2-224053 (CONET) and by the Science and Technology Foundation of Portugal (FCT). We thank Claro Noda and Jasper Büsch for helping as the subjects of some of the experiments.

References

1. Buettner, M., Yee, G.V., Anderson, E., Han, R.: X-MAC: a short preamble MAC protocol for duty-cycled wireless sensor networks. In: SenSys '06: Proceedings of the 4th International Conference on Embedded Networked Sensor Systems. pp. 307–320. ACM, New York, NY, USA (2006)
2. Cai, J., Cheng, S., Huang, C.: MAC channel model for WBAN. Tech. Rep. 15-09-0562-00-0006, IEEE P802.15 (July 2009)
3. Chen, K., Muhlethaler, P.: A scheduling algorithm for tasks described by time value function. Real-Time Syst. 10(3), 293–312 (May, 1996)
4. Chipcon Corporation: CC2420 2.4 GHz IEEE 802.15.4 / ZigBee-ready RF Transceiver. `http://www.ti.com/lit/gpn/cc2420` (Apr 2002)
5. van Dam, T., Langendoen, K.: An adaptive energy-efficient MAC protocol for wireless sensor networks. In: SenSys '03: Proceedings of the 1st International Conference on Embedded Networked Sensor Systems. pp. 171–180. ACM, New York, NY, USA (2003)
6. Davenport, D., Ross, F., Deb, B.: Wireless propagation and coexistence of medical body sensor networks for ambulatory patient monitoring. In: Wearable and Implantable Body Sensor Networks, International Workshop on. pp. 109–113. IEEE Computer Society, Los Alamitos, CA, USA (2009)
7. El-Hoiydi, A., Decotignie, J.D.: Low power downlink MAC protocols for infrastructure wireless sensor networks. Mob. Netw. Appl. 10(5), 675–690 (2005)
8. Gaertner, G., ONuallain, E., Butterly, A., Singh, K., Cahill, V.: 802.11 link quality and its prediction an experimental study. In: Niemegeers, I., de Groot, S.H. (eds.) Personal Wireless Communications. Lecture Notes in Computer Science, vol. 3260, pp. 609–611. Springer Berlin / Heidelberg (2004)
9. Ghaddar, M., Talbi, L., Denidni, T.: Human body modelling for prediction of effect of people on indoor propagation channel. Electronics Letters 40(25), 1592 – 1594 (Dec 2004)
10. Guerra, R., Fohler, G.: A gravitational task model with arbitrary anchor points for target sensitive real-time applications. Real-Time Syst. 43(1), 93–115 (2009)
11. Halkes, G.P., Van Dam, T., Langendoen, K.G.: Comparing energy-saving MAC protocols for wireless sensor networks. Mob. Netw. Appl. 10(5), 783–791 (2005)
12. Hanson, M.A., Powell Jr., H.C., Barth, A.T., Ringgenberg, K., Calhoun, B.H., Aylor, J.H., Lach, J.: Body area sensor networks: Challenges and opportunities. Computer 42, 58–65 (2009)
13. Hauer, J.H., V.Handziski, A.Wolisz: Experimental study of the impact of wlan interference on IEEE 802.15.4 body area networks. In: Proc. of 6th European Conference on Wireless Sensor Networks (EWSN). Cork, Ireland (Feb 2009)
14. Jensen, E.D., Locke, C.D., Tokuda, H.: A time-driven scheduling model for real-time operating systems. In: RTSS' 85: Proc. of the 6th IEEE Real-Time Systems Symposium. pp. 112 – 122. IEEE Press, Los Alamitos, CA (1985)
15. Kara, A., Bertoni, H.: Blockage/shadowing and polarization measurements at 2.45 ghz for interference evaluation between Bluetooth and IEEE 802.11 WLAN. Antennas and Propagation Society International Symposium, 2001. IEEE 3, 376–379 vol.3 (2001)
16. Liu, S., Fan, K.W., Sinha, P.: CMAC: an energy-efficient MAC layer protocol using convergent packet forwarding for wireless sensor networks. ACM Trans. Sen. Netw. 5(4), 1–34 (2009)

17. Miluzzo, E., Zheng, X., Fodor, K., Campbell, A.T.: Radio characterization of 802.15.4 and its impact on the design of mobile sensor networks. In: EWSN'08: Proceedings of the 5th European conference on Wireless sensor networks. pp. 171–188. Springer-Verlag, Berlin, Heidelberg (2008)
18. Obayashi, S., Zander, J.: A body-shadowing model for indoor radio communication environments. Antennas and Propagation, IEEE Transactions on 46(6), 920–927 (Jun 1998)
19. Polastre, J., Hill, J., Culler, D.: Versatile low power media access for wireless sensor networks. In: SenSys '04: Proceedings of the 2nd International Conference on Embedded Networked Sensor Systems. pp. 95–107. ACM, New York, NY, USA (2004)
20. Rajendran, V., Obraczka, K., Garcia-Luna-Aceves, J.J.: Energy-efficient collision-free medium access control for wireless sensor networks. In: SenSys '03: Proc. of the 1st International Conference on Embedded Networked Sensor Systems. pp. 181–192. ACM Press, New York, NY, USA (2003)
21. Ravindran, B., Jensen, E.D., Li, P.: On recent advances in time/utility function real-time scheduling and resource management. In: Object-Oriented Real-Time Distributed Computing, IEEE International Symposium on. pp. 55–60. IEEE Computer Society, Los Alamitos, CA, USA (2005)
22. Rhee, I., Warrier, A., Aia, M., Min, J.: Z-MAC: a hybrid MAC for wireless sensor networks. In: SenSys '05: Proc. of the 3rd International Conference on Embedded Networked Sensor Systems. pp. 90–101. ACM Press, New York, NY, USA (2005)
23. Sentilla Corporation: Tmote sky datasheet. `http://www.sentilla.com/pdf/eol/tmote-sky-datasheet.pdf`
24. Shimmer Research: Shimmer2 capabilities overview. `http://www.shimmer-research.com/wp-content/uploads/2010/08/Shimmer-2R-C%apabilities-Overview.pdf`
25. Srinivasan, K., Levis, P.: RSSI is under appreciated. In: Proceedings of the Third Workshop on Embedded Networked Sensors (EmNets06) (2006)
26. U.S. Health Resources and Services Administrations: What is Behind HRSA's Projected Supply, Demand, and Shortage of Registered Nurses? `http://bhpr.hrsa.gov/healthworkforce/reports/behindrnprojections/index.%htm` (Sep 2004)
27. Wang, J., Ravindran, B.: Time-utility function-driven switched ethernet: Packet scheduling algorithm, implementation, and feasibility analysis. IEEE Transactions on Parallel and Distributed Systems 15, 119–133 (2004)
28. Ye, W., Heidemann, J., Estrin, D.: Medium access control with coordinated adaptive sleeping for wireless sensor networks. IEEE/ACM Trans. Netw. 12(3), 493–506 (2004)
29. Ye, W., Silva, F., Heidemann, J.: Ultra-low duty cycle MAC with scheduled channel polling. In: SenSys '06: Proceedings of the 4th international conference on embedded networked sensor systems. pp. 321–334. ACM, New York, NY, USA (2006)
30. Yoo, S.M., Chen, C.J., Chou, P.H.: Low-complexity, high-throughput multiple-access wireless protocol for body sensor networks. In: Wearable and Implantable Body Sensor Networks, International Workshop on. pp. 109–113. IEEE Computer Society, Los Alamitos, CA, USA (2009)